Chapter 4

NNLO Analysis of Gluon Distribution Function in the DGLAP Approach

4.1 Introduction

The gluon distribution function is one of the extremely indispensable physical observables that controls the physics at high energy or small-x in DIS, where x is the Bjorken variable. Especially, precise knowledge of gluon distribution functions at small-x is of utmost importance in estimating backgrounds and exploring new physics at the Large Hadron Collider. The gluon distribution $G(x, Q^2)$ does not come into sight in the experimentally available proton structure function $F_2(x, Q^2)$. It is determined only via the quark distributions together with the evolution equations. More direct approach to determine the gluon distribution is based on the reconstruction of the kinematics of the interacting partons from the measurement of the hadronic final state in gluon induced processes. They are controlled by different systematic effects and provide a substantive test of perturbative QCD. The proton structure function is measured by the H1 and ZEUS collaboration at HERA [1-3] over a wide kinematic region which makes it possible to know about the gluon distribution in the previously unexplored region of x and Q^2. The fast growth of the proton structure function at small-x observed at HERA brings about much attention because perturbative QCD in conjunction with the DGLAP equation [4-7] attributes this sharp growth to a similar rise of gluon density towards small-x. In the DGLAP formalism the gluon

distribution turns out to be very large at small-x and so it contributes crucially to the evolution of the parton distribution. Subsequently, the gluon distribution governs the structure function $F_2(x, Q^2)$ through the evolution $g \to q\bar{q}$ in the small-x region. In this situation it is very important to explore the possibility of obtaining analytical solutions of DGLAP equations at least in the restricted domain of small-x and many approximated analytical solutions of the gluon distribution function in the framework of DGLAP equation have been reported in recent years with significant phenomenological success [8-14].

In this chapter, we derive an explicit expression for the gluon distribution function upto NNLO by solving the DGLAP evolution equation for gluon distribution function analytically. In such an approach, we use a Taylor series expansion valid at small-x and reframes the DGLAP equations as partial differential equations in the variables x and Q^2 as discussed in chapter 3. The resulting equations at LO, NLO and NNLO are then solved by the Lagrange's auxiliary method to obtain the Q^2 and x-evolutions of the gluon distribution function. The obtained results can be described within the framework of perturbative QCD. To illustrate the method and check the compatibility of our predicted gluon distributions, we use the published values of the gluon distributions from the GRV1998NLO [15], MRST2004NNLO [16], MSTW2008NNLO [17] and JR09NNLO [18] global analyses. We find that the analytic gluon distributions from our solution are consistent with these parametrizations. We also compare our results with the Block-Durand-McKay (BDM) model [14] and observe that our results depict almost the same behaviour as that of BDM model.

4.2 Formalism

4.2.1 General framework

The DGLAP evolution equation for gluon distribution function in the standard form is given by [19]

$$\frac{\partial g(x,Q^2)}{\partial \ln Q^2} = \int_x^1 \frac{d\omega}{\omega}\Big(P_{gq}(\omega)q_S(x/\omega,Q^2) + P_{gg}(\omega)g(x/\omega,Q^2)\Big), \tag{4.1}$$

where the splitting function P_{gq} is defined as

$$\begin{aligned} P_{gq}(x,Q^2) &= \frac{\alpha_s(Q^2)}{2\pi}P_{gq}^{(0)}(x) + \Big(\frac{\alpha_s(Q^2)}{2\pi}\Big)^2 P_{gq}^{(1)}(x) + \Big(\frac{\alpha_s(Q^2)}{2\pi}\Big)^3 P_{gq}^{(2)}(x) \\ &\quad + \mathcal{O}P_{gq}^{(3)}(x). \end{aligned} \tag{4.2}$$

where $P_{gq}^{(0)}(x)$, $P_{gq}^{(1)}(x)$ and $P_{gq}^{(2)}(x)$ are LO, NLO and NNLO quark-gluon splitting functions respectively. The gluon-gluon splitting function P_{gg} can be defined in a Similar fashion. Here q_S is the singlet quark density and g is the gluon density. The representation $G(x,Q^2) = xg(x,Q^2)$ is used here.

4.2.2 LO analysis of gluon distribution function

Substituting the explicit form of the LO splitting functions [7, 21] in Eq.(4.1) and simplifying, the LO DGLAP evolution equation for the gluon distribution function can be written as

$$\frac{\partial G(x,t)}{\partial t} = \frac{\alpha_s(t)}{2\pi}\Big[6\Big(\frac{11}{12} - \frac{N_f}{18} + \ln(1-x)\Big)G(x,t) + 6I_1^g(x,t)\Big], \tag{4.3}$$

where $G(x,Q^2) = xg(x,Q^2)$ is the gluon distribution function. The integral function $I_1^g(x,t)$ is defined as

$$\begin{aligned} I_1^g(x,t) &= \int_x^1 d\omega\Bigg[\frac{\omega G\big(\frac{x}{\omega},t\big) - G(x,t)}{1-\omega} + \Big(\omega(1-\omega) + \frac{1-\omega}{\omega}\Big)G\Big(\frac{x}{\omega},t\Big) \\ &\quad + \frac{2}{9}\Bigg(\frac{1+(1-\omega)^2}{\omega}\Bigg)F_2^S(\frac{x}{\omega}t).\Bigg] \end{aligned} \tag{4.4}$$

Here the variable t is used where $t = \ln(Q^2/\Lambda^2)$. Now, using Taylor expansion method and neglecting higher order terms of x, since we consider the small-x ($x < 0.1$) domain in our analysis, as discussed in the Chapter-3, we can write $G(x/\omega,t)$ as

$$G\Big(\frac{x}{\omega},t\Big) = G(x,t) + \frac{xu}{1-u}\frac{\partial G(x,t)}{\partial x}. \tag{4.5}$$

Similarly, $F_2^S(\frac{x}{\omega},t)$ can be approximated as

$$F_2^S\Big(\frac{x}{\omega},t\Big) = F_2^S(x,t) + \frac{xu}{1-u}\frac{\partial F_2^S(x,t)}{\partial x}. \tag{4.6}$$

Substituting these values of $G(\frac{x}{\omega},t)$ and $F_2^S(\frac{x}{\omega},t)$ in Eq.(4.4) and carrying out the integrations in u we get from Eq.(4.3)

$$\begin{aligned} \frac{\partial G(x,t)}{\partial t} &= \frac{6A_f}{t}\Big[A_1^g(x)G(x,t) + A_2^g(x)\frac{\partial G(x,t)}{\partial x} + A_3^g(x)F_2^S(x,t) \\ &\quad + A_4^g(x)\frac{\partial F_2^S(x,t)}{\partial x}\Big], \end{aligned} \tag{4.7}$$

where $A_i^g(x)$ (i=1,2,3,4) are functions of x (see Appendix D). $\frac{A_f}{t} = \frac{\alpha_s(t)}{2\pi}$ where $A_f = \frac{2}{\beta_0}$ and β_0 is the one-loop correction to the QCD beta function. Eq.(4.7) is a partial differential equation for gluon distribution function with respect to the

variables x and t. Thus using a Taylor expansion valid at small-x we reframe the DGLAP equation for gluon distribution, which is an integro-differential equation, as partial differential equation in two variables x and t or Q^2.

The gluon distribution is coupled to the singlet structure function and therefore to obtain an analytical solution of the DGLAP evolution equation for gluon distribution function a relation between gluon distribution function and singlet structure function has to be assumed. As discussed in chapter 3, here also we assume the relation $G(x,t) = K(x)F_2^S(x,t)$ [22-24] to solve Eq.(4.7) where $K(x)$ is a parameter to be determined from phenomenological analysis. From this relation we get $F_2^S(x,t) = K_1(x)G(x,t)$, where $K_1(x) = 1/K(x)$. Using this relation Eq.(4.7) takes the form

$$-t\frac{\partial G(x,t)}{\partial t} + L_1^g(x)\frac{\partial G(x,t)}{\partial x} + M_1^g(x)G(x,t) = 0, \tag{4.8}$$

with

$$L_1^g(x) = 6A_f\Big[A_2^g(x) + K_1(x)A_4^g(x)\Big], \tag{4.9}$$

$$M_1^g(x) = \frac{12}{\beta_0}\Big[A_1^g(x) + K_1(x)A_3^g(x) + \frac{\partial K_1(x)}{\partial x}A_4^g(x)\Big], \tag{4.10}$$

Now the general solution of the equation (4.8) is

$$F(U,V) = 0, \tag{4.11}$$

where $F(U,V)$ is an arbitrary function of U and V. Here, $U(x,t,G(x,t)) = k_1$ and $V(x,t,G(x,t)) = k_2$ are two independent solutions of the Lagrange's equation

$$\frac{\partial x}{L_1^g(x)} = \frac{\partial t}{-t} = \frac{\partial G(x,t)}{-M_1^g(x)G(x,t)}. \tag{4.12}$$

Solving Eq. (4.12) we obtain

$$U(x,t,G(x,t)) = t\cdot\exp\Big[\int\frac{1}{L_1^g(x)}dx\Big] \tag{4.13}$$

and

$$V(x,t,G(x,t)) = G(x,t)\cdot\exp\Big[\int\frac{M_1^g(x)}{L_1^g(x)}dx\Big]. \tag{4.14}$$

Thus we see that it has no unique solution. In this approach we attempt to extract a particular solution that obeys some physical constraints on the structure

function. The simplest possibility to get a solution is that a linear combination of U and V should obey the Eq.(4.11) so that

$$\alpha \cdot U + \beta \cdot V = 0, \tag{4.15}$$

where α and β are arbitrary constants to be determined from the boundary conditions on singlet structure function. Putting the values of U and V from Eq.(4.13) and Eq.(4.14) respectively in Eq.(4.15) we get

$$\alpha t \cdot \exp\Big[\int \frac{1}{L_1^g(x)}dx\Big] + \beta G(x,t) \cdot \exp\Big[\int \frac{M_1^g(x)}{L_1^g(x)}dx\Big] = 0, \tag{4.16}$$

which implies,

$$G(x,t) = -\gamma t \cdot \exp\Big[\int \Big(\frac{1}{L_1^g(x)} - \frac{M_1^g(x)}{L_1^g(x)}\Big)dx\Big] \tag{4.17}$$

where $\gamma = \frac{\alpha}{\beta}$ is another constant. Now at $t = t_0$, where $t_0 = \ln\frac{Q_0^2}{\Lambda^2}$ for any lower value $Q^2 = Q_0^2$, we define

$$G(x,t_0) = -\gamma t_0 \cdot \exp\Big[\int (\frac{1}{L_1^g(x)} - \frac{M_1^g(x)}{L_1^g(x)})dx\Big]. \tag{4.18}$$

Then Eqs.(4.17) and (4.18) lead us to

$$G(x,t) = G(x,t_0)\Big(\frac{t}{t_0}\Big). \tag{4.19}$$

This gives the t or Q^2-evolution ($t = \ln(Q^2/\Lambda^2)$) for gluon distribution function at LO at a particular value small-x. Again we define

$$G(x_0,t) = -\gamma t \cdot \exp\Big[\int (\frac{1}{L_1^g(x)} - \frac{M_1^g(x)}{L_1^g(x)})dx\Big]_{x=x_0}, \tag{4.20}$$

at a higher value of $x = x_0$. Then from Eq.(4.17) and Eq.(4.20) we get

$$G(x,t) = G(x_0,t) \cdot \exp\Big[\int_{x_0}^{x} (\frac{1}{L_1^g(x)} - \frac{M_1^g(x)}{L_1^g(x)})dx\Big]. \tag{4.21}$$

which gives the x-evolutions of gluon distribution function at LO for a given value of Q^2.

4.2.3 NLO analysis of gluon distribution function

Substituting the NLO splitting functions [25-27] in Eq.(4.1) and simplifying, we get the DGLAP equation for gluon distribution function at NLO in standard form as

$$\begin{aligned}\frac{\partial G(x,t)}{\partial t} &= \frac{\alpha_s(t)}{2\pi}\Big[6\Big(\frac{11}{12} - \frac{N_f}{18} + \ln(1-x)\Big)G(x,t) + 6I_1^g(x,t)\Big] \\ &\quad + \Big(\frac{\alpha_S(t)}{2\pi}\Big)^2 I_2^g(x,t),\end{aligned} \tag{4.22}$$

where the integral function $I_2^g(x,t)$ is defined as

$$I_2^g(x,t) = \int_x^1 d\omega \Big[P_{gg}^1(\omega) G\big(\frac{x}{\omega}, t\big) + A(\omega) F_2^S\Big(\frac{x}{\omega}, t\Big)\Big] \tag{4.23}$$

The explicit forms of $P_{gg}^1(\omega)$ and $A(\omega)$ are given in Appendix E.

Following the same procedure as in LO, the Eq.(4.22) can be simplified as

$$-\Big(\frac{t^2}{t - b\ln t}\Big)\frac{\partial G(x,t)}{\partial t} + L_2^g(x)\frac{\partial G(x,t)}{\partial x} + M_2^g(x) G(x,t) = 0. \tag{4.24}$$

Here

$$L_2^g(x) = \frac{2}{\beta_0}\Big[6\Big(A_2^g(x) + K_1(x)A_4^g(x)\Big) + T_0\Big(B_2^g(x) + K_1(x)B_4^g(x)\Big)\Big], \tag{4.25}$$

$$\begin{aligned} M_2^g(x) &= \frac{2}{\beta_0}\Big[6\Big(A_1^g(x) + K_1(x)A_3^g(x) + \frac{\partial K_1(x)}{\partial x}A_4^g(x)\Big) \\ &\quad + T_0\Big(B_1^g(x) + K_1(x)B_3^g(x) + \frac{\partial K_1(x)}{\partial x}B_4^g(x)\Big)\Big], \end{aligned} \tag{4.26}$$

where $B_i^g(x)$, (i=1,2,3,4) are functions of x (see Appendix D). Here we consider the numerical parameter T_0 such that $T^2(t) = T_0 T(t)$ where $T(t)$=$\frac{\alpha_S(t)}{2\pi}$. As discussed in chapter 3, this parameter is chosen in such a way that the difference between $T^2(t)$ and $T_0T(t)$ is negligible in the specified range under study.

Thus proceeding in the same way we solve Eq.(4.24) we obtain the t or Q^2 and x-evolutions of gluon distribution function at NLO as

$$G(x,t) = G(x,t_0)\Big(\frac{t^{1+b/t}}{t_0^{1+b/t_0}}\Big)\cdot\exp\Big(\frac{b}{t} - \frac{b}{t_0}\Big) \tag{4.27}$$

and

$$G(x,t) = G(x_0,t)\cdot\exp\Big[\int_{x_0}^{x}\big(\frac{1}{L_2^g(x)} - \frac{M_2^g(x)}{L_2^g(x)}\big)dx\Big] \tag{4.28}$$

with $b = \frac{\beta_1}{\beta_0^2}$. The input functions $G(x,t_0)$ and $G(x_0,t)$ can be determined by applying the initial conditions at $t = t_0$ as well as at $x = x_0$ as in the previous case.

4.2.4 NNLO analysis of gluon distribution function

Using the splitting functions upto NNLO [28-30] and simplifying, we get the DGLAP equations for gluon distribution function at NNLO as

$$\begin{aligned} \frac{\partial G(x,t)}{\partial t} &= \frac{\alpha_s(t)}{2\pi}\Big[6\Big(\frac{11}{12} - \frac{N_f}{18} + \ln(1-x)\Big)G(x,t) + 6I_1^g(x,t)\Big] \\ &\quad + \Big(\frac{\alpha_S(t)}{2\pi}\Big)^2 I_2^g(x,t) + \Big(\frac{\alpha_S(t)}{2\pi}\Big)^3 I_3^g(x,t), \end{aligned} \tag{4.29}$$

where, the integral functions I_3^g is given by

$$I_3^g(x,t) = \int_x^1 d\omega \Big[P_{gg}^2(\omega) G\Big(\frac{x}{\omega}, t\Big)\Big]. \tag{4.30}$$

The explicit forms of the function P_{gg}^2 is given in Appendix F. In this case we overlook the quark contribution to the gluon distribution function. The reason behind this approximation is that at very small values of x, the gluons, being the most abundant parton, dominate over the quarks. Moreover, it simplifies the calculations involving the NNLO splitting functions which otherwise are very complicated to solve analytically.

To obtain an analytical solution of Eq.(4.29) we consider the numerical parameter T_1 such that $T^3(t) = T_1 T(t)$, where $T(t)$=$\frac{\alpha_S(t)}{2\pi}$. The value of T_1 is determined by phenomenological analysis, like T_0, from a particular range of Q^2 under study and by an appropriate choice of T_1 the error can be reduced to a minimum. Thus Eq. (4.29) can be simplified as

$$-\Big(\frac{t^2}{t - b\ln t + b^2(\ln^2 t - \ln t - 1) + c}\Big) + L_3^g(x)\frac{\partial G(x,t)}{\partial x} + M_3^g(x) G(x,t) = 0. \tag{4.31}$$

Here

$$\begin{aligned} L_3^g(x) &= \frac{2}{\beta_0}\Big[6\Big(A_2^g(x) + K_1(x)A_4^g(x)\Big) + T_0\Big(B_2^g(x) + K_1(x)B_4^g(x)\Big) \\ &\quad + T_1 C_2^g(x)\Big], \end{aligned} \tag{4.32}$$

$$\begin{aligned} M_3^g(x,t) &= \frac{2}{\beta_0}\Big[6\Big(A_1^g(x) + K_1(x)A_3^g(x) + \frac{\partial K_1(x)}{\partial x}A_4^g(x)\Big) + T_0\Big(B_1^g(x) \\ &\quad + K_1(x)B_3^g(x) + \frac{\partial K_1(x)}{\partial x}B_4^g(x)\Big) + T_1 C_1^g(x)\Big], \end{aligned} \tag{4.33}$$

where $C_i^g(x)$, (i=1,2) are functions of x (see Appendix D).

Following the same procedure as earlier, we solve Eq.(4.31) and obtain the t or Q^2 and x-evolutions of gluon distribution function at NNLO as

$$G(x,t) = G(x,t_0)\Big(\frac{t^{1+(b-b^2)/t}}{t_0^{1+(b-b^2)/t_0}}\Big) \cdot \exp\Big(\frac{b - c - b^2\ln^2 t}{t} - \frac{b - c - b^2\ln^2 t_0}{t_0}\Big) \tag{4.34}$$

and

$$G(x,t) = G(x_0,t) \cdot \exp\Big[\int_{x_0}^{x} \Big(\frac{1}{L_3^g(x)} - \frac{M_3^g(x)}{L_3^g(x)}\Big)dx\Big], \tag{4.35}$$

where $b = \frac{\beta_1}{\beta_0^2}$ and $c = \frac{\beta_2}{\beta_0^3}$. The input functions $G(x,t_0)$ and $G(x_0,t)$ can be determined by applying the initial conditions at $t = t_0$ as well as at $x = x_0$ as earlier.

4.3 Result and discussion

In this chapter, obtain the Q^2 or t ($t = \ln(Q^2/\Lambda^2)$) and x-evolutions of the gluon distribution function solving the DGLAP evolution equation for gluon density up to NNLO approximation. The analysis is performed in the range $5 \leq Q^2 \leq 110$ GeV^2 and $10^{-4} \leq x \leq 0.1$. The computed results of gluon distribution function at LO, NLO and NNLO are compared with the available GRV1998NLO [15], MRST2004NNLO [16], MSTW2008NNLO [17] and JR09NNLO [18] global QCD analysis. We also compare our results with the results of the BDM model [14]. The BDM model obtains an analytic solution for the LO gluon distribution function directly from the proton structure function using the accurate Froissart-bound [31] type parametrization of proton structure function. In this model, it is shown that using an analytic expression that successfully reproduces the known experimental data for proton structure function in a domain $x_{min}(Q^2) \leq x \leq x_{max}(Q^2)$ and $Q^2_{min} \leq Q^2 \leq Q^2_{max}$ in DIS, the gluon distribution $G(x, Q^2)$ can be uniquely determined in the same domain of x and Q^2. In all the graphs, the lowest-Q^2 and highest-x points are taken as input for

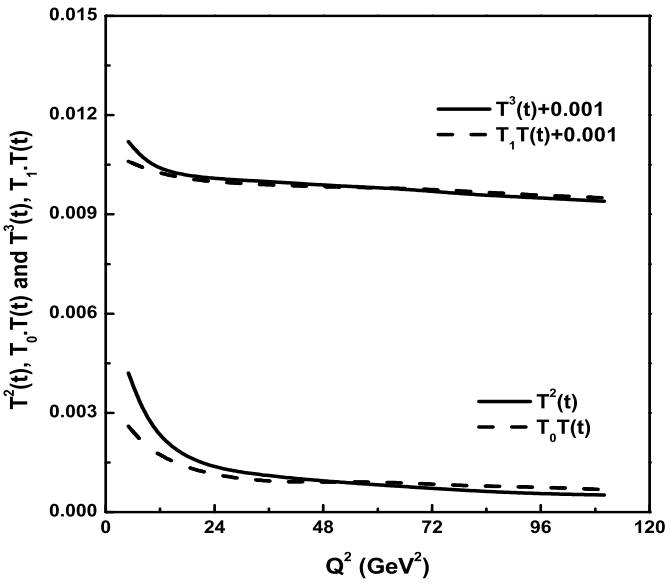

Figure 4.1: Comparison of T^2 and $T_0.T(t)$ as well as T^3 and $T_1.T(t)$ versus Q^2.

$G(x, t_0)$ and $G(x_0, t)$ respectively. As mentioned earlier for the analytical solution of DGLAP equation for gluon distribution function we consider a function $K_1(x)$ which relates the gluon distribution and the singlet structure function. For simplicity we consider the function $K_1(x) = K_1$, where K_1 is a constant parameter. The acceptable

range of the arbitrary constant K_1 is found to be $0.14 \leq K_1 \leq 0.85$. In each figure the dot lines represent our LO results, the dash-dot lines represent our NLO results whereas the solid lines represent the NNLO results. As expected the improvement is found to be better at NNLO than at NLO and LO.

In the calculation of gluon distribution function at NLO and NNLO, we consider two numerical parameters T_0 and T_1 to linearise the equations in α_s as discussed in section 4.2. These numerical parameters are obtained for a particular range of Q^2 under study. Figure 4.1 shows the plot of $T^2(t)$ and $T_0T(t)$ as well as $T^3(t)$ and $T_1T(t)$ versus Q^2 in the range $2 < Q^2 < 110$ GeV^2. It is observed that for $T_0 = 0.035$ and $T_1 = 0.0042$ the differences between $T^2(t)$ and $T_0T(t)$ as well as $T^3(t)$ and $T_1T(t)$ becomes negligible in the Q^2 range under study. Therefore, the consideration of the parameters T_0 and T_1 does not induce any unexpected change in our results.

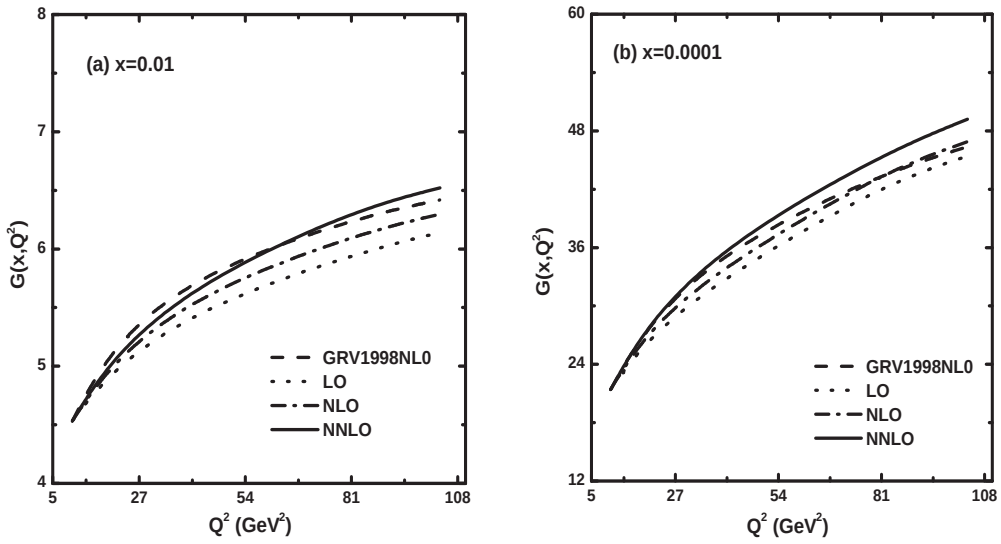

Figure 4.2: Q^2 evolution of gluon distribution functions at LO, NLO and NNLO compared with GRV1998NLO for two fixed values x. The dot lines represent the LO results (Eq.4.19), dash-dot lines represent the NLO results (Eq.4.27) and solid lines represent the NNLO results Eq.(4.34).

Figure 4.2 and Figure 4.3 show the comparison of the analytical gluon distributions obtained by solving the DGLAP equation for gluon distribution at LO, NLO and NNLO with the published results of GRV1998NLO. In Figure 4.2 we plot the computed values of $G(x, Q^2)$ from Eqs.(4.19), (4.27) and (4.34) for LO, NLO and NNLO respectively vs. Q^2 at $x = 0.01$ and $x = 0.0001$ respectively in the range $10 \leq Q^2 \leq 105$ Gev^2. It is seen from the figures that the predictions at NNLO

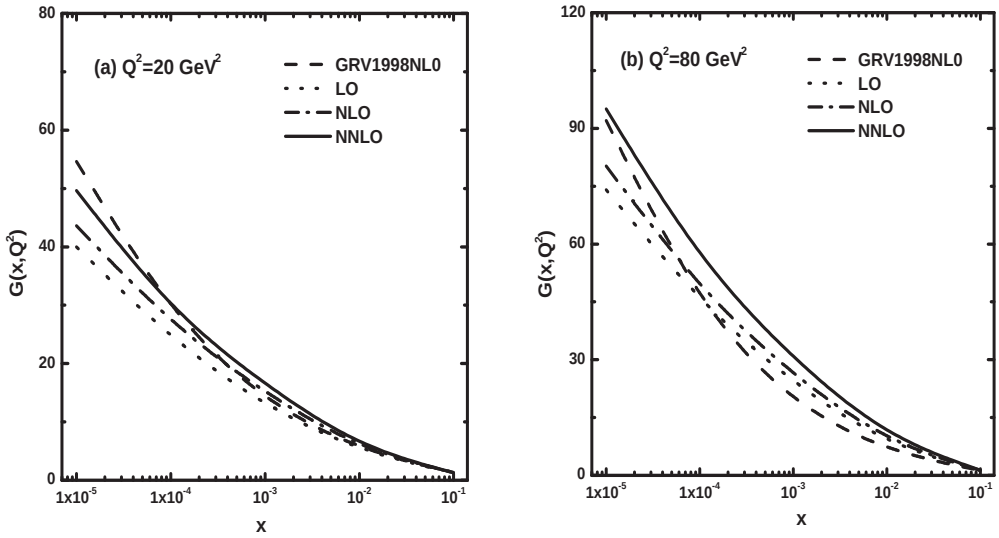

Figure 4.3: x evolution of gluon distribution functions at LO, NLO and NNLO compared with GRV1998NLO data for two fixed Q^2. The dot lines represent the LO results (Eq.4.21), dash-dot lines represent the NLO results (Eq.4.28) and solid lines represent the NNLO results Eq.(4.35).

approximation show better agreement with the GRV results at $x = 0.01$. On the other hand in Figure 4.3 the computed values of $G(x, Q^2)$ obtained from Eqs.(4.21), (4.28) and (4.35) for LO, NLO and NNLO respectively are plotted against x for two representative Q^2, viz. $Q^2 = 20\ GeV^2$ and $Q^2 = 80\ GeV^2$ respectively in the range $10^{-4} \leq x \leq 0.1$.

Figure 4.4 represent the comparison of our results of Q^2 or t ($t = \ln(Q^2/\Lambda^2)$) evolution of gluon distribution function $G(x, Q^2)$ calculated from Eqs.(4.19), (4.27) and (4.34) for LO, NLO and NNLO respectively with the MRST2004NNLO global analysis. Here we plot our predictions of $G(x, Q^2)$ as functions of Q^2 for some fixed values of x, viz. at $x = 0.01, 0.001, 0.0005$ and 0.0001 considering the Q^2 domain $5 \leq Q^2 \leq 100$ GeV^2. The NNLO predictions show the better compatibility with MRST2004 result particularly at $x = 0.001$.

In Figure 4.5 we plot our computed results of gluon distribution $G(x, Q^2)$ obtained from Eqs.(4.21), (4.28) and (4.35) for LO, NLO and NNLO respectively as functions of x for $Q^2 = 20, 40, 60$ and 80 GeV^2 respectively. Here we compare our results with the MRST2004NNLO predictions in the x range $10^{-4} \leq x \leq 0.1$. The NNLO approximation improves the agreement of the predicted values of $G(x, Q^2)$ with MRST2004NNLO global analysis.

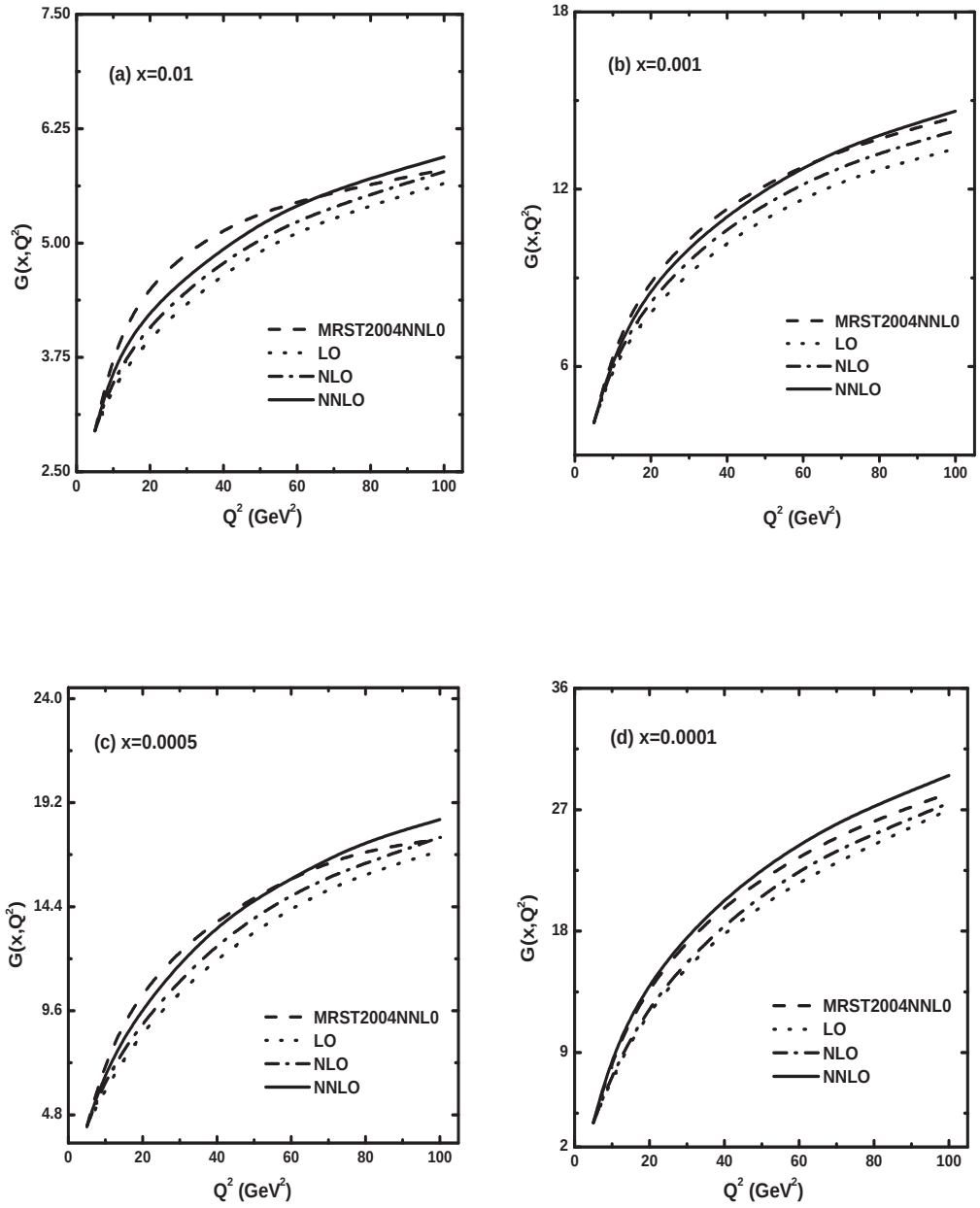

Figure 4.4: Comparison of Q^2 evolution of gluon distribution functions at LO, NLO and NNLO with MRST2004NNLO parametrization for four fixed values x. The dot lines represent the LO results (Eq.4.19), dash-dot lines represent the NLO results (Eq.4.27) and solid lines represent the NNLO results Eq.(4.34).

Figure 4.6 depict the Q^2-evolution of $G(x, Q^2)$ at LO, NLO and NNLO obtained from Eqs. (4.19), (4.27) and (4.34) respectively in the range $5 \leq Q^2 \leq 105$ GeV^2. Here our predictions are compared with the MSTW2008NNLO parametrization and the comparison is performed for four fixed x values, namely x=0.01, 0.005, 0.001 and 0.0001. For each x, the NNLO result show good consistency with the MSTW2008NNLO predictions.

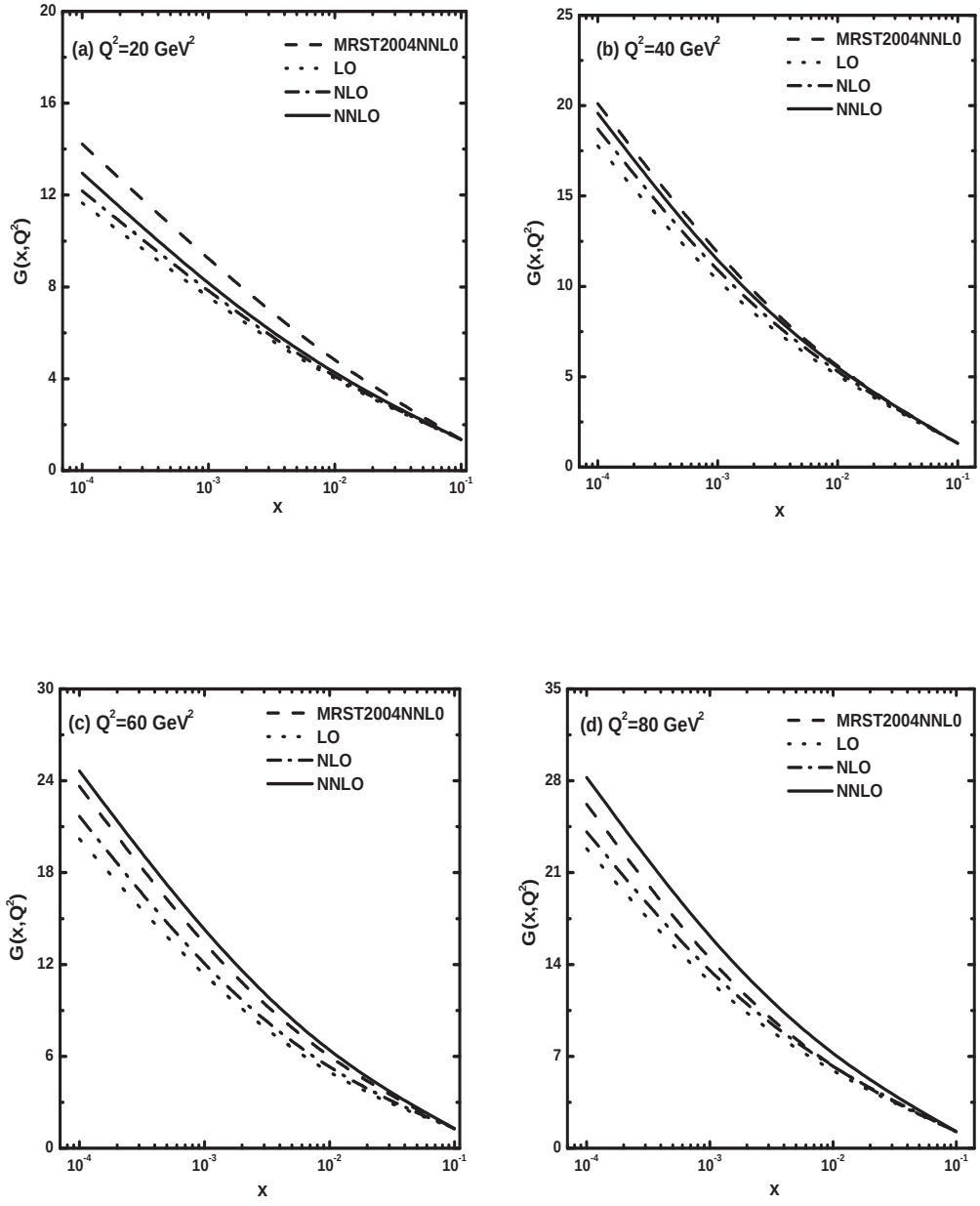

Figure 4.5: Comparison of the values of gluon distribution function at LO, NLO and NNLO plotted against x with the MRST2004NNLO parametrization for four representative Q^2. The dot lines represent the LO results (Eq.4.21), dash-dot lines represent the NLO results (Eq.4.28) and solid lines represent the NNLO results Eq.(4.35).

Figure 4.7 shows the comparison of our results of x-evolutions of $G(x, Q^2)$ at LO, NLO and NNLO obtained from Eqs.(4.21), (4.28) and (4.35) with those obtained by the MSTW2008NNLO parametrization in the range $10^{-4} \leq x \leq 0.1$. The comparison is done for four representative $Q^2 = 30, 50, 80$ and 100 GeV^2. It can be seen that the NNLO result for each Q^2 agrees well with the MSTW2008NNLO parametrization.

We also compare the predicted results of x dependence of gluon distribution

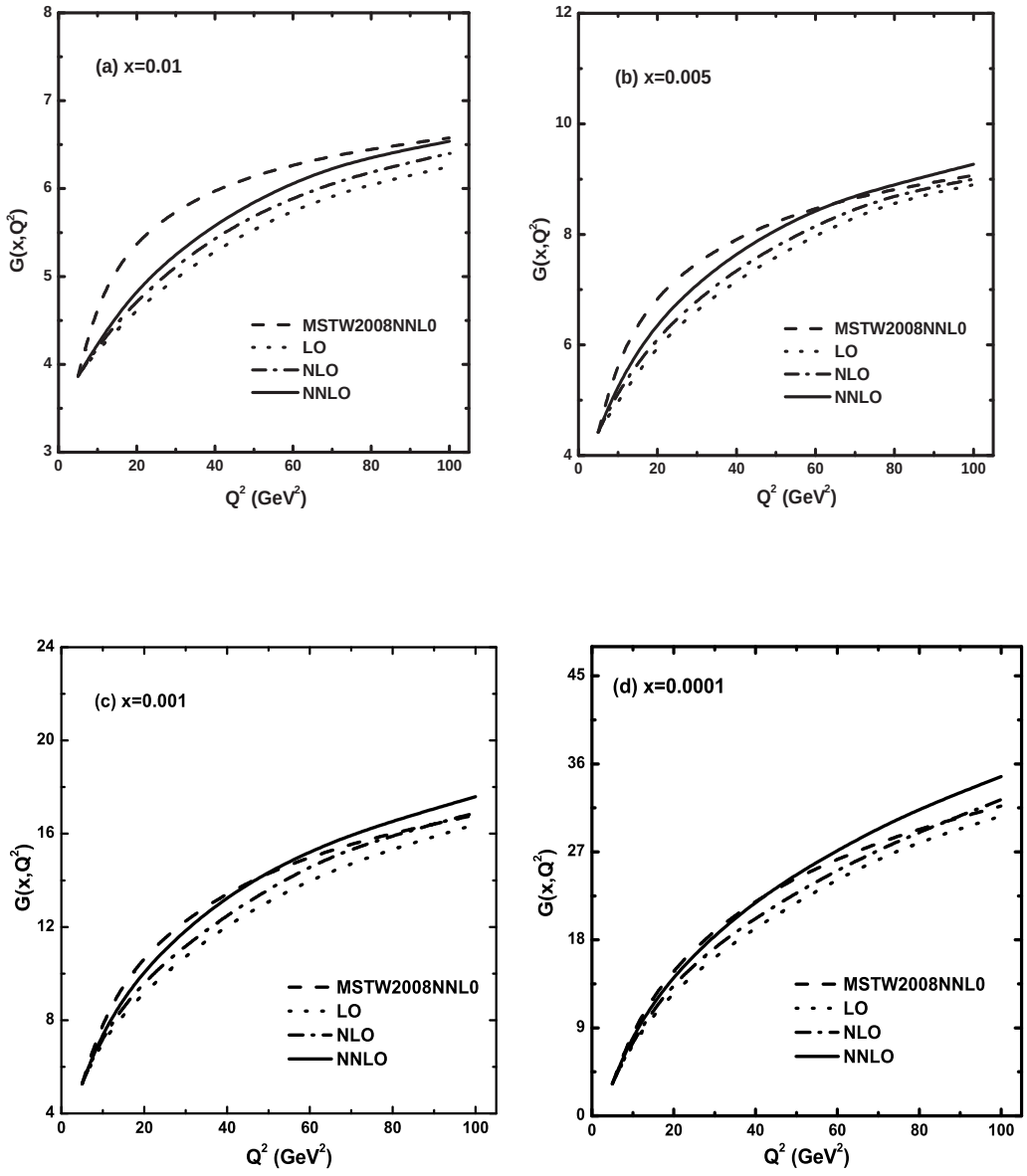

Figure 4.6: Q^2 evolution of gluon distribution function at LO, NLO and NNLO compared with MSTW2008NNLO parametrization for four fixed x values. The dot lines represent the LO results (Eq.4.19), dash-dot lines represent the NLO results (Eq.4.27) and solid lines represent the NNLO results Eq.(4.34).

function $G(x, Q^2)$ with the JR09NNLO global parton analysis [18] as well as with the results of BDM model [14]. This comparison is portrayed in Figure 4.8 where we plot the computed values of $G(x, Q^2)$ at LO, NLO and NNLO using Eqs. (4.26), (4.33) and (4.40) versus x in the range $10^{-4} \leq x \leq 0.1$ for $Q^2 = 5$ GeV^2 and $Q^2 = 20$ GeV^2. Our predictions of $G(x, Q^2)$ at NNLO show very good agreement with the JR09NNLO. Our results also show similar behaviour with those of BDM model, however the BDM

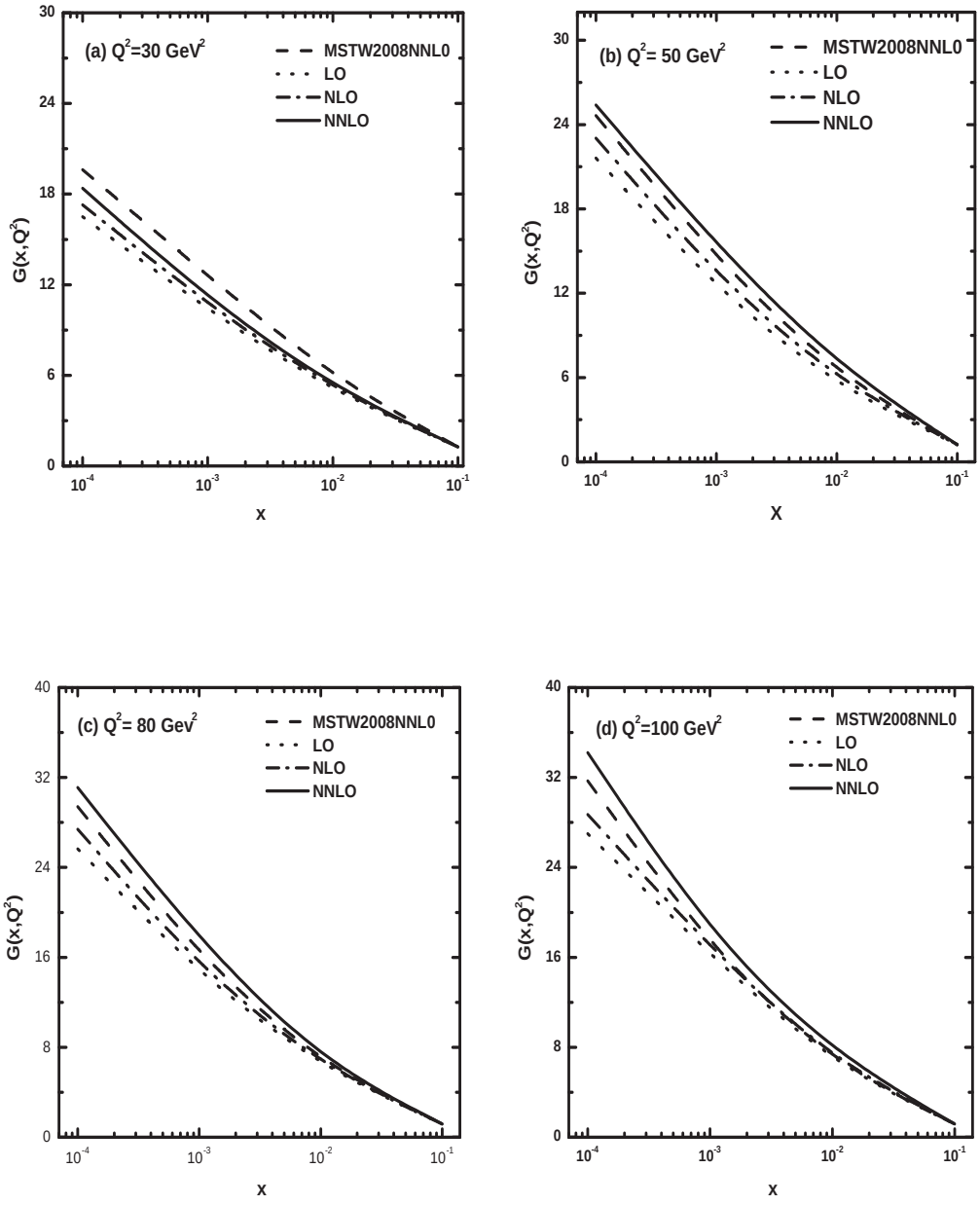

Figure 4.7: Comparison of the values of gluon distribution function at LO, NLO and NNLO plotted against x with the MSTW2008NNLO parametrization for four representative Q^2. The dot lines represent the LO results (Eq.4.21), dash-dot lines represent the NLO results (Eq.4.28) and solid lines represent the NNLO results Eq.(4.35).

model gives much larger gluon distribution towards small x. Figures indicate that the compatibility of our predictions with the JR09NNLO parametrization much better that that of BDM model.

To check the compatibility of our results of gluon distribution function at LO, NLO and NNLO respectively with different parametrizations, we perform a χ^2 test shown in Table 4.1. From this we observe that our results are almost comparable

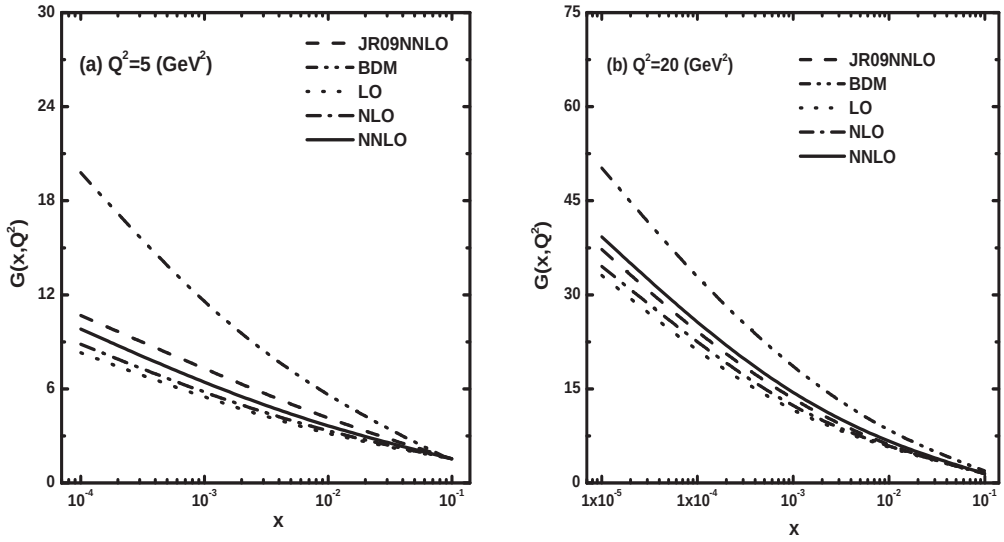

Figure 4.8: Comparison of our predictions of gluon distribution function at LO, NLO and NNLO with JR09NNLO global fit as well as with the BDM model for two representative Q^2. The dot lines are the LO results of obtained from Eq.(4.21), dash-dot lines are NLO results from Eq.(4.28) and solid lines are the NNLO results from Eq.(4.35). The dash curves are from the JR09NNLO parametrization and dash-dot-dot curves are the results of BDM model.

Table 4.1: χ^2 text for $G(x, Q^2)$

Order	**GRV1998**	**MRST2004**	**MSTW2008**	**JR09**
LO	4.03	2.34	3.18	2.38
NLO	3.16	1.63	2.16	1.24
NNLO	2.96	0.85	1.72	0.61

with different parametrizations and the inclusion of NNLO contributions improve the consistency.

4.4 Summary

To summarise the evolution of gluon distribution function with respect to x and Q^2 at LO, NLO and NNLO are presented by solving the DGLAP evolution equation for gluon distribution analytically. Here the DGLAP equation is first transformed into a partial differential equation in the two variables x and Q^2 by using the Taylor series expansion valid at small-x. Following this the resulting equation is solved at LO, NLO and NNLO respectively by the Lagrange's auxiliary method to obtain the Q^2 and x evolutions of the gluon distribution function. We compare our predictions with the GRV1998NLO, MRST2004NNLO, MSTW2008NNLO and JR09NNLO global QCD

analysis as well as with the BDM model. The obtained results of gluon distribution can be described within the framework of perturbative QCD. Our results show that at fixed x the gluon distribution function increases with increasing Q^2, whereas at fixed Q^2 it increases as x decreases which is in agreement with perturbative QCD fits at small-x. We perform our analysis in the Q^2 and x range, viz. $5 \leq Q^2 \leq 110$ GeV^2 and $10^{-4} \leq x \leq 0.1$ and note that in this domain our predicted solutions are comparable with different global analysis of parton distributions. We consider the function $K_1(x) = K_1$, where K_1 is a constant parameter, in defining the relation between gluon and singlet structure functions and obtain our best fitted results in the range $0.14 \leq K_1 \leq 0.85$. Moreover we consider the numerical parameters T_0 and T_1 to linearise the equations at NLO and NNLO in α_s. These parameters are chosen from phenomenological analysis for a particular range of Q^2 under study and therefore, the use of the parameters T_0 and T_1 does not produce any abrupt change in our results. From our phenomenological analysis we observe that our computed results of gluon distribution function at NNLO show significantly better agreement with different parameterizations than those of LO and NLO. Thus we can say that the NNLO approximation has appreciable contribution to the gluon distribution function in the particular range of x and Q^2 under study. However, in the very small-x region, where the number density of gluons become very high, the gluon recombination processes may take place inducing nonlinear corrections to the QCD evolution and in that case the solution suggested in this chapter may not be sufficient to explain the available data at very small-x. The nonlinear GLR-MQ evolution equation may provide a good description of the high density QCD at very small-x, which we will discuss in the next chapter.

Bibliography

[1] Adloff, C. et al., On the rise of the proton structure function F_2 towards low x, *Phys. Lett. B* **520** (3-4), 183−−190, 2001.

[2] Adloff, C. et al., Deep-inelastic inclusive *ep* scattering at low x and a determination of α_s, *Eur. Phys. J. C* **21**(1), 33−−61 2001.

[3] Chekanov, S. et al., Measurement of the neutral current cross section and F_2 structure function for deep inelastic e^+p scattering at HERA, *Eur. Phys. J. C* **21**(3),443−−471, 2001.

[4] Gribov, V. N., Lipatov, L. N. Deep inelastic *ep* scattering in perturbation theory, *Sov. J. Nucl. Phys.* **15**(4), 438−−450, 1972.

[5] Gribov, V. N., Lipatov, L. N. e^+e^- pair annihilation and deep-inelastic *ep* scattering in perturbation theory, *Sov. J. Nucl. Phys.* **15**(4), 675−−684, 1972.

[6] Dokshitzer, V. Calculation of structure functions of deep-inelastic scattering and e^+e^- annihilation by perturbation theory in quantum chromodynamics, *Sov. Phys. JETP* **46**(4), 641−−652, 1977.

[7] Altarelli, G., Parisi, G. Asymptotic freedom in parton language, *Nucl. Phys. B* **126**(2), 298−−318, 1977.

[8] Prytz, K. Approximate determination of the gluon density at low-x from the F_2 scaling violations, *Physics Letters B* **311**(1-4), 286−−290, 1993.

[9] Prytz, K. An approximate next-to-leading order relation between the low-x F_2 scaling violations and the gluon density, *Phys. Lett. B* **332**(3-4), 393−−397, 1994.

[10] Sarma, J. K., Medhi, G. K. Regge behaviour of structure function and gluon distribution at low-x in leading order, *Eur. Phys. J. C* **16**(3), 481487, 2000.

[11] Choudhury, D. K., Deka, Ranjita and Saikia, A. Gluon distribution and $\frac{dF_2}{d\ln Q^2}$ at small x in the next-to-leading order, *Eur. Phys. J. C* **2**(2), 301−−305, 1998.

[12] Choudhury, D. K., Sahariah, P. K. A solution of the DGLAP equation for gluon at low x, *Pramana J. Phys.* **58**(4), 599−−610, 2002.

[13] Choudhury, D. K., Sahariah, P. K. The next-to-leading order (NLO) gluon distribution from DGLAP equation and the logarithmic derivatives of the proton structure function $F_2(x, Q^2)$ at low x, *Pramana J. Phys.* **65**(2), 193−−213, 2005.

[14] Block, Martin M., Durand, Loyal and McKay, Douglas W. Analytic derivation of the leading-order gluon distribution function $G(x, Q^2)$ from the proton structure function $F_2^p(x, Q^2)$, *Phys. Rev. D* **77**(9), 094003, 2008.

[15] Gluck, M., Reya, E. and Vogt, A. Dynamical parton distributions revisited, *Eur. Phys. J. C* **5**(3), 461−−470, 1998.

[16] Martin, A. D. et al., Physical gluons and high-ET jets, *Physics Letters B* **604**(1-2), 61−−68, 2004.

[17] Martin, A. D. et al., Parton distributions for the LHC, *Eur. Phys. J. C* **63**(2), 189−−285, 2009.

[18] Jimenez-Delgado, P., Reya, E. Dynamical NNLO parton distributions, *Phys. Rev. D* **79**(7), 074023, 2009.

[19] Van Neerven, W. L., Vogt, A. NNLO evolution of deep-inelastic structure functions: the singlet case, *Nucl. Phys. B* **588**(1-2), 345−−373, 2000.

[20] Shaikhatdenov, B. G. et al., QCD coupling constant at next-to-next-to-leading order from DIS data, *Phys. Rev. D* **81**(3), 034008, 2010.

[21] Abbott, L. F., Atwood, W. B. and Michael Barnett, R. Quantum-chromodynamic analysis of eN deep-inelastic scattering data, *Phys. Rev.* **22**(3), 582−−594, 1980.

[22] Sarma, J. K., Das, B. t evolutions of structure functions at low-x, *Phys. Lett. B* **304**(3-4), 323−−328, 1993.

[23] Sarma, J. K., Choudhury, D. K. and Medhi, G. K. x-distribution of deuteron structure function at low-x, *Phys.Lett. B* **403**(1-2), 139−−144, 1997.

[24] Baishya, R., Sarma, J. K. Method of characteristics and solution of DGLAP evolution equation in leading and next to leading order at small x, *Phys. Rev. D* **74**(10), 107702, 2006.

[25] Furmanski, W., Petronzio, R. Lepton-hadron processes beyond leading order in quantum chromodynamics, *Z. Phys. C* **11**(4), 293−−314, 1982.

[26] Furmanski, W., Petronzio, R. Singlet parton densities beyond leading order, *Phys.Lett. B* **97**(3-4), 437−−442, 1980.

[27] Curci, G., Furmanski, W. and Petronzio, R. Evolution of parton densities beyond leading order: The non-singlet case, *Nucl. Phys. B* **175**(1), 27−−92, 1981.

[28] Van Neerven, W. L., Vogt, A. NNLO evolution of deep-inelastic structure functions: the singlet case, *Nucl. Phys. B* **588**(1-2), 345−−373, 2000.

[29] Vogt, A., Moch, S. and Vermaseren, J. A. M. The three-loop splitting functions in QCD: the singlet case, *Nucl. Phys. B* **691**(1-2), 129−−181, 2004.

[30] Ellis, R. K., Kunszt, Z. and Levina, E. M. The evolution of parton distributions at small x, *Nuclear Physics B* **420**(3), 517−−549, 1994.

[31] Froissart, M. Asymptotic Behavior and Subtractions in the Mandelstam Representation, *Phys. Rev.* **123**(3), 1053−−1057, 1961.